Chapter 8. Cloud Thermal Structure

Notes:

- *Most of the material presented in this chapter is taken from Stahler and Palla (2004), Chap. 8.*

8.1 The Buildup of Molecules

In order for molecules to form in the interior there must be something, or some process, that will eliminate any substantial radiation that may dissociate any newly formed molecule. This is especially true for molecular hydrogen where the process of **self-shielding** will allow the formation of molecules deeper in the cloud, away from harmful ultraviolet radiation. We now wish to explain the observed density and atomic/molecular structure depicted in Figure 8.1.

8.1.1 The Atomic Envelope

We assume that no stellar X-ray radiation is present, which implies that gas heating can only be provided by cosmic rays (equations (7.50 and (7.51) and photoelectric ejection from dust grains (equation (7.53); due to ultraviolet radiation). Carbon ionization cannot provide heating, as most of the atomic carbon will already be ionized, while dust irradiation does not heat the gas. Comparison of equations (7.50), (7.51), and (7.53) reveals that the latter dominates over the other two.

On the other hand, comparing the relevant cooling process and their associated rates (i.e., equations (7.56) to (7.59)) we find that cooling through ionized carbon fine structure excitation will be dominant. We can, therefore, write

$$\Gamma_{\rm PE} = \Lambda_{\rm CI}$$

$$3\times10^{-11}\left(\frac{n_{\rm H}}{10^3\ {\rm cm}^{-3}}\right)\ {\rm eV\ cm^{-3}s^{-1}} = 3\times10^{-9}\left(\frac{n_{\rm H}}{10^3\ {\rm cm}^{-3}}\right)^2 e^{-\frac{92\ {\rm K}}{T_{\rm g}}}\ {\rm eV\ cm^{-3}s^{-1}}, \tag{8.1}$$

and determine the density dependent gas temperature with

$$T_{\rm g} = \frac{40\ {\rm K}}{2.0 + \log\left(n_{\rm H}/10^3\ {\rm cm}^{-3}\right)}. \tag{8.2}$$

We found in Chapter 2 (Section 2.1.5) that an examination of the properties of the different components populating the interstellar medium, except for the molecular gas, revealed an interesting fact. That is, when we calculate the quantity $nT = P/k_{\rm B}$ (P is the pressure), we found values that all approach a few times 1,000 cm^{-3} K to better than a factor of two or three. This fact leads us to the idea that the different phases of the interstellar medium are in pressure equilibrium. Although this notion will not apply to the interior of molecular clouds where the pressure will increase greatly, it does apply for the edge of clouds, i.e., the atomic component.

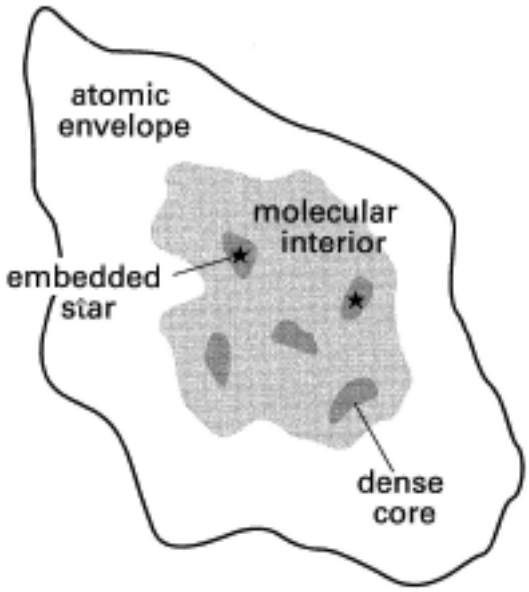

Figure 8.1 – Depiction of density and atomic/molecular structure of a typical molecular cloud.

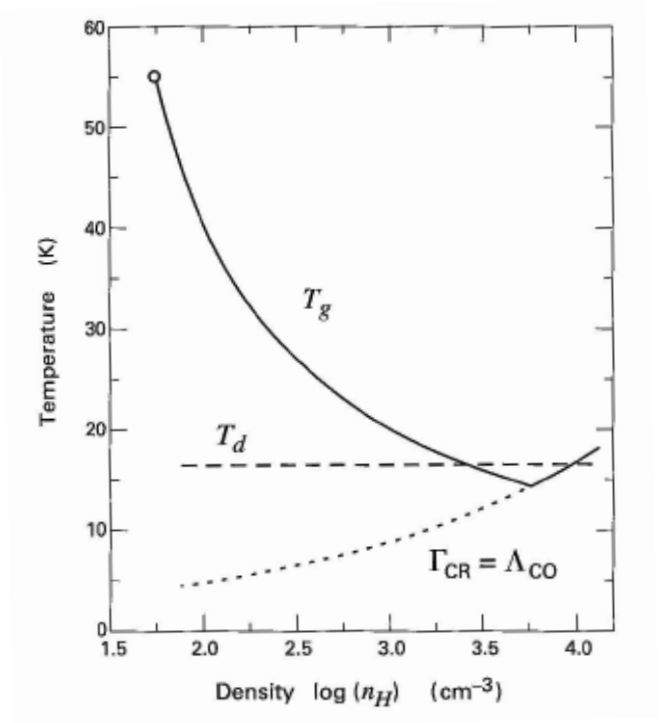

Figure 8.2 – Temperature profiles for the gas and dust in the lower-density regions of a molecular cloud. The open circle depicts the conditions at the boundary of the cloud, in the atomic envelope, when pressure equilibrium with the interstellar medium is attained.

Choosing a mean value of $n_{\rm H}T_{\rm g} \simeq 3{,}000$ cm^{-3}K we can verify from equations (8.1) or (8.2) that $n_{\rm H} = 56$ cm^{-3} and $T_{\rm g} = 54$ K. This condition is shown as an open circle in Figure 8.2, as well the gas temperature- density relation given in equation (8.2).

It is also interesting to estimate the temperature of the dust population. To do, we first come to the realization that of all of the processes that can heat the grains (i.e., equations (7.53) and (7.54)) dust irradiation will dominate. For equilibrium to be attained this heating rate must be equalized by cooling through thermal emission (equation (7.59)). Equating the corresponding equations we find that the dust temperature is constant at

$$T_{\rm d} = 16.5 \text{ K}. \tag{8.3}$$

The dust is therefore significantly cooler than the gas in the atomic envelope; this is also shown in Figure 8.2.

8.1.2 **Molecular Hydrogen Abundance**

As we progress deeper into the cloud, the temperature of the gas goes down and $\rm H_2$ molecules will tend form on the surface of dust grains (and be ejected back to the gas afterwards). Of course, these newly formed molecules are at risk of being destroyed by incident ultraviolet radiation. But if we go far enough into the cloud, these photons will be fewer and fewer, as the $\rm H_2$ molecules and the dust grains populating the upper layers will efficiently absorb them. The photon depletion due to $\rm H_2$ absorption is called **self-shielding**.

If $\sigma_i(\nu)$ is the cross-section characterizing the interaction between a photon of frequency ν with a $\rm H_2$ molecule, which is initially in its electronic ground state (but not necessarily rovibrational ground state) but then subsequently excited to one of the next two electronic states, we can write the **volumetric dissociation rate** as

$$\begin{aligned} \mathcal{D}_{\rm H_2} &= 4\pi n_{\rm H_2} \sum_i \beta_i \int \frac{J_\nu}{h\nu} \sigma_i(\nu) d\nu \\ &= 4\pi n_{\rm H_2} \sum_i \frac{\beta_i J_{\nu_i}}{h\nu_i} \int \sigma_i(\nu) d\nu, \end{aligned} \tag{8.4}$$

where we took advantage of the fact that $\sigma_i(\nu)$ varies much faster than J_ν with frequency. In equation (8.4) β_i is the probability that the subsequent decay from the corresponding excited electronic state leads to the dissociation of the molecule, and

$$J_\nu \equiv \frac{1}{4\pi} \int I_\nu \, d\Omega, \tag{8.5}$$

is the average specific intensity (see equation 2.19 of the lecture notes). Dividing both sides of equation (8.4) by the molecular hydrogen number density yields the inverse of the dissociation time

$$t_{\rm diss}^{-1} = 4\pi \sum_i \frac{\beta_i J_{\nu_i}}{h\nu_i} \int \sigma_i(\nu) d\nu, \tag{8.6}$$

and

$$\mathcal{D}_{\rm H_2} = n_{\rm H_2} t_{\rm diss}^{-1}. \tag{8.7}$$

If there is no self-shielding, i.e., at the edge of the atomic envelope, then the different values J_{ν_i} are those for the interstellar radiation field (see Figure 7.4 of Stahler and Palla). It can be found in this case the $t_{\rm diss}^{-1} \simeq 400$ yr. We note that

$$\nu_i \approx 3\times 10^{15} \text{ Hz} \tag{8.8}$$

and

$$\int \sigma_i(\nu) d\nu \approx 1\times 10^{-4} \text{ cm}^2\text{s}^{-1}. \tag{8.9}$$

We recall from Chapter 5 that volumetric formation rate of $\rm H_2$ is given by

$$\begin{aligned} \mathcal{R}_{\rm H_2} &= \frac{1}{2}\gamma_{\rm H} n_{\rm d} \nu_{\rm c} \\ &= \frac{1}{2}\gamma_{\rm H} n_{\rm d} n_{\rm H} |v_r| \sigma_{\rm d}, \end{aligned} \tag{8.10}$$

where $\gamma_{\rm H} \simeq 0.3$ is the sticking probability of a hydrogen atom to the surface of the grain. The mean relative velocity between the dust grains and hydrogen atom $|v_r|$ is given by

$$|v_r| = \left(\frac{3\mathcal{R}T_{\rm g}}{2\mu} \right)^{1/2}. \tag{8.11}$$

In the atomic envelope we set $\mu = 1.3$ for the mean mass number of a gas particle and $T_{\rm g} = 54$ K for the gas temperature. We can then calculate the **molecular fraction**

$$f_{\rm H_2} \equiv \frac{2n_{\rm H_2}}{n_{\rm H}} \tag{8.12}$$

by equating the destruction and formation rates of equations (8.7) and (8.10), respectively. Doing so, we find that

$$\begin{aligned} f_{\mathrm{H}_2} &= \gamma_{\mathrm{H}} n_{\mathrm{d}} |v_r| \sigma_{\mathrm{d}} t_{\mathrm{diss}} \\ &= \gamma_{\mathrm{H}} \Sigma_{\mathrm{d}} n_{\mathrm{HI}} |v_r| t_{\mathrm{diss}} \\ &= 3 \times 10^{-5}, \end{aligned} \tag{8.13}$$

where we used equation (2.44) for Σ_{d} the total geometric cross-section of dust per hydrogen atom ($\Sigma_{\mathrm{d}} = 1.1 \times 10^{-21}$ cm^2 from equation (2.48), and $n_{\mathrm{HI}} \simeq 56$ cm^{-3}. We therefore find that the density of molecular hydrogen is very low at the edge of a cloud with $n_{\mathrm{H}_2} \simeq 8.4 \times 10^{-4}$ cm^{-3}.

As we go deeper in the cloud we must take into account the fact that the dust that also populates these regions can also absorb the radiation. We therefore define the total optical depth at a given frequency as

$$\tau(\nu) = N_{\mathrm{H}} \Sigma_{\mathrm{d}} + N_{\mathrm{H}_2} \sigma_i(\nu), \tag{8.14}$$

where the first term is due to the presence of dust, which is composed of grains of size assumed to be much larger than the wavelength of radiation. We can now generalized equation (8.4) for the dissociation rate to

$$\begin{aligned} \mathcal{D}_{\mathrm{H}_2} &= 4\pi n_{\mathrm{H}_2} \sum_i \beta_i \int \frac{J_\nu e^{-\tau(\nu)}}{h\nu} \sigma_i(\nu) d\nu \\ &= 4\pi n_{\mathrm{H}_2} e^{-N_{\mathrm{H}} \Sigma_{\mathrm{d}}} \sum_i \frac{\beta_i J_{\nu_i}}{h\nu_i} \int \sigma_i(\nu) e^{-N_{\mathrm{H}_2} \sigma_i(\nu)} d\nu, \end{aligned} \tag{8.15}$$

where we have assumed a plane-parallel slab for the geometry of the system.

We can further modify equation (8.15) because of the aforementioned realization that the cross-section $\sigma_i(\nu)$ has a finite extent in frequency, as is made evident by any observed spectral line profile (see Problem 1 of the Second assignment, for example). Accordingly, the **normalized line profile** $\phi(\nu - \nu_i)$, centered on the frequency ν_i, to express the cross-section as follows

$$\sigma_i(\nu) = \phi(\nu - \nu_i) \int \sigma_i(\nu') d\nu', \tag{8.16}$$

with

$$\int \phi(\nu - \nu_i) d\nu \equiv 1. \tag{8.17}$$

We thus write

$$\mathcal{D}_{\mathrm{H}_2} = 4\pi n_{\mathrm{H}_2} e^{-N_{\mathrm{H}}\Sigma_{\mathrm{d}}} \sum_i \frac{\beta_i J_{\nu_i} \delta_i}{h\nu_i} \int \sigma_i(\nu) d\nu, \tag{8.18}$$

with the **penetration probability** δ_i for a photon to penetrate a column density N_{H_2} defined as

$$\delta_i \equiv \int \phi(\nu - \nu_i) e^{-N_{\mathrm{H}_2}\phi(\nu-\nu_i)\int \sigma_i(\nu')d\nu'} d\nu. \tag{8.19}$$

It should be clear that the likeliness that a photon penetrates to a given distance Δr (for a specified volume density; $\Delta r = N_{\mathrm{H}_2} / n_{\mathrm{H}_2}$) decreases with the (column) density.

The details of the line profile are likely to vary from one region to another. But in order to gain some insights as to the level of photon penetration as a function of the column density we will assume that the line profiles are **Lorentzian** in nature. More precisely, we express the normalized line profile with the so-called **Lorentz profile function**

$$\phi(\nu - \nu_i) = \frac{\gamma_i / 4\pi^2}{(\nu - \nu_i)^2 + (\gamma_i / 4\pi^2)^2}, \tag{8.20}$$

where γ_i corresponds to the Einstein coefficient for spontaneous emission, which was assumed to be such that $\gamma_i \ll \nu - \nu_i$ in the last equation ($\gamma_i \approx 10^9$ s^{-1} whereas $\nu_i \approx 10^{15}$ Hz; see equation (8.8)). One of the characteristics of the Lorentz profile is that it exhibits significant **line wings** away from the **line core** where the intensity in highest. The presence of such high velocity wings is very common in line profiles observed in the turbulent regions of molecular clouds.

It should also be clear that photons that have a frequency that lies within the line core have a smaller penetration probability (for a given column density) than photons whose frequency fall in the wings of the line. For example, if we concentrate on those photons with frequencies located in a range $\Delta\nu$ well within the line core such that we crudely approximate

$$\phi(\nu - \nu_i) \approx 1/\Delta\nu, \tag{8.21}$$

then inserting this relation into equation (8.19) yields

$$\delta_i \approx e^{-N_{\mathrm{H}_2} \int \sigma(\nu')d\nu' / \Delta\nu}. \tag{8.22}$$

It is apparent from this equation that the penetration probability in the line core is negligible when the exponent is on the order of unity (or more). We therefore define the corresponding column density ΔN_{H_2} with

$$\Delta N_{\mathrm{H}_2} = \frac{\Delta\nu}{\int \sigma(\nu) d\nu}. \tag{8.23}$$

On the other hand, when we consider only photons with frequencies located out in the line wings we can approximate equation (8.20) with

$$\phi(\nu - \nu_i) \approx \frac{\gamma_i}{4\pi^2 (\nu - \nu_i)^2}. \tag{8.24}$$

Insertion into equation (8.19) we find (the combination of our approximation, i.e., equation (8.24), and the exponential in the penetration probability function implies that we more or less neglect the contribution of the line core in the following, as we should)

$$\begin{aligned}
(\delta_i)^2 &= \left[\frac{\gamma_i}{4\pi^2} \int \frac{e^{-\frac{N_{\mathrm{H}_2}\gamma_i}{4\pi^2(\nu-\nu_i)^2}\int \sigma_i(\nu')d\nu'}}{(\nu-\nu_i)^2} d\nu \right]^2 \\
&= \left[\frac{\gamma_i}{4\pi^2} \int e^{-\frac{N_{\mathrm{H}_2}\gamma_i(\omega-\omega_i)^2}{4\pi^2}\int \sigma_i(\nu')d\nu'} d\omega \right]^2 \\
&= \left(\frac{\gamma_i}{4\pi^2} \right)^2 2\pi \int_0^\infty e^{-\frac{N_{\mathrm{H}_2}\gamma_i\rho^2}{4\pi^2}\int \sigma_i(\nu')d\nu'} \rho d\rho \\
&= \left(\frac{\gamma_i}{4\pi^2} \right)^2 \frac{(2\pi)^3}{N_{\mathrm{H}_2}\gamma_i \int \sigma_i(\nu') d\nu'},
\end{aligned} \tag{8.25}$$

where $\omega = 1/\nu$ and we went from a two-dimensional frequency system to corresponding polar coordinates (we also assumed that $-\infty < \nu < \infty$ instead of $0 < \nu < \infty$, which is a reasonable approximation considering the typical values for ν_i in comparison to the width of the line profile). We finally combine equations (8.22) and (8.25) to write

$$\delta_i \approx \begin{cases} e^{-N_{\mathrm{H}_2}/\Delta N_{\mathrm{H}_2}}, & N_{\mathrm{H}_2} \lesssim \Delta N_{\mathrm{H}_2} \\ \left(\dfrac{N_i}{N_{\mathrm{H}_2}} \right)^{1/2}, & N_{\mathrm{H}_2} \gtrsim \Delta N_{\mathrm{H}_2} \end{cases} \tag{8.26}$$

with

$$\Delta N_{\mathrm{H}_2} \approx \left(\frac{v_i}{c}\right)\frac{\Delta V}{\int \sigma(\nu)d\nu}$$
$$N_i = \frac{\gamma_i}{2\pi\int \sigma(\nu)d\nu}, \tag{8.27}$$

where ΔV is the line width in velocity unit. If we choose $\Delta V = 1\ \mathrm{km\ s^{-1}}$, we then find that $\Delta N_{\mathrm{H}_2} \approx 10^{14}\ \mathrm{cm^{-3}}$, and with $\gamma_i \approx 10^9\ \mathrm{s^{-1}}$ and considering equation (8.9) we find that $N_i \approx 10^{12}\ \mathrm{cm^{-2}}$. We see from equations (8.26) that the initial strong attenuation in the photon penetration probability is due to the line core (for $n_{\mathrm{H}_2} \sim 100\ \mathrm{cm^{-3}}$ the column density ΔN_{H_2} is reached at a depth of approximately only 10^{12} cm or $\sim 10^{-6}$ pc), while the existence of the remaining dissociating photons comes from the presence of the line wings.

It should not be forgotten, however, that dust also contributes in reducing the dissociation rate by contributing an additional exponential factor in equation (8.18). Accordingly, keeping equation (8.6) for the inverse of the dissociation time and equating the relations for the dissociation (i.e., equation (8.18)) and the formation rates (i.e., equation (8.10)) we find that deep in the interior of a cloud (where the penetration probability is set by the line wings)

$$\begin{aligned}\frac{n_{\mathrm{H}_2}}{t_{\mathrm{diss}}}\frac{\langle N_i\rangle^{1/2}}{N_{\mathrm{H}_2}^{1/2}}e^{-N_{\mathrm{H}}\Sigma_{\mathrm{d}}} &= \frac{1}{2}\gamma_{\mathrm{H}} n_{\mathrm{d}} n_{\mathrm{H}} |v_r|\sigma_{\mathrm{d}} \\ &= \frac{1}{2}\gamma_{\mathrm{H}}\Sigma_{\mathrm{d}} n_{\mathrm{HI}} n_{\mathrm{H}} |v_r| \\ &= \frac{1}{2}\gamma_{\mathrm{H}}\Sigma_{\mathrm{d}} n_{\mathrm{H}}\left(n_{\mathrm{H}} - 2n_{\mathrm{H}_2}\right)|v_r|,\end{aligned} \tag{8.28}$$

where

$$\frac{\langle N_i\rangle^{1/2}}{N_{\mathrm{H}_2}^{1/2}} = \frac{\sum_i \frac{\beta_i J_{\nu_i}\delta_i}{h\nu_i}\int \sigma_i(\nu)d\nu}{\sum_i \frac{\beta_i J_{\nu_i}}{h\nu_i}\int \sigma_i(\nu)d\nu} \tag{8.29}$$

is the average of the penetration probability over the different absorption lines. We can find the column density of molecular hydrogen associated with the penetration distance in the cloud Δr with the following integral

$$N_{\mathrm{H}_2} \equiv \int_0^{\Delta r} n_{\mathrm{H}_2} d(\Delta r), \tag{8.30}$$

which from equation (8.28) must equal

$$N_{H_2} = \frac{4\langle N_i \rangle e^{-2n_H \Sigma_d \Delta r}}{\left[\gamma_H t_{diss} \Sigma_d n_H \left(n_H / n_{H_2} - 2\right)|v_r|\right]^2}. \tag{8.31}$$

Equations (8.30) and (8.31) can combined to solve for the molecular fraction f_{H_2} and the ultraviolet dust optical depth $\tau \equiv n_H \Sigma_d \Delta r$. The result is shown in Figure 8.3 in the (unlikely) case where n_H is uniform across the cloud at 100 cm^{-3} and $T_g = 30$ K.

A similar build up process occurs for CO, even though this molecular does not form primarily on the surface of dust grains like molecular hydrogen. Instead this molecule forms through reactions involving the C^+ ion (please note that this is not the case in dense cores (see equations (5.12) to (5.15) of the lecture notes), but only in regions of lower densities where molecules build up). So in this case the formation rate of CO would be dependent on the ionization rate of carbon and the following chemical reactions

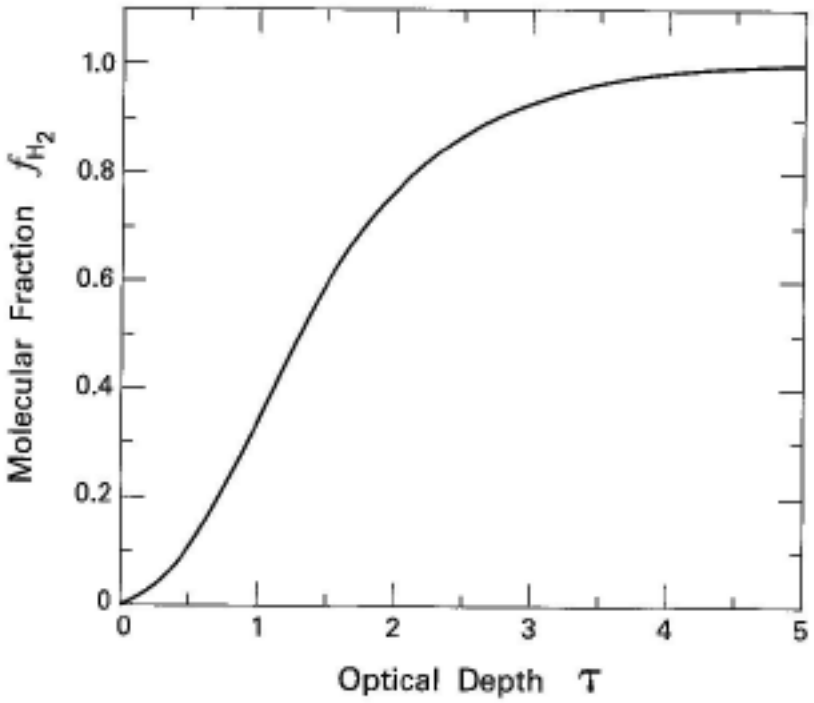

Figure 8.3 – The molecular fraction f_{H_2} in the interior of a molecular cloud as a function of the ultraviolet dust optical depth.

$$\begin{aligned} C^+ + H_2 &\rightarrow CH_2^+ \\ CH_2^+ + e^- &\rightarrow CH + H \\ CH + O &\rightarrow CO + H, \end{aligned} \tag{8.32}$$

for example. Once CO is formed, it will self-shield itself in the same manner as H_2. A schematic for the abundance of these two molecules as a function of the depth in the cloud (measured through the visual extinction) is shown in Figure 8.4.

8.2 The Molecular Interior

As we enter the interior of a molecular cloud where the populations of the main molecular species (e.g., H_2 and CO) have built up (where $A_V \sim 1$), there will be little to no radiation field left to ionize the gas. The main source of ionization will then reside with the cosmic rays that can penetrate deep into the interior of clouds. Moreover, the cosmic rays are also the only significant source of heating. Assuming that some sort of equilibrium is reached, inspection of equations (7.56) to (7.60) reveals that CO collisional excitation will be the dominant source of cooling for the gas. We then write

$$\Gamma_{CR}(H_2) = \Lambda_{CO}^*. \tag{8.33}$$

Solving for T_g after equating equations (7.51) and (7.58) yields the rising curve shown in Figure 8.2. If we go further in the interior to the sufficiently high densities that defines dense cores (i.e., $n_H \gtrsim 10^4$ cm^{-3} and A_V is very large), however, the collisions between the gas molecules and the dust grains are frequent enough that heat can be efficiently transferred to the dust, if it is cooler than the gas. Equation (8.33) must then be modified to

$$\Gamma_{CR}(H_2) = \Lambda_{CO}^* + \Lambda_{g\rightarrow d}. \tag{8.34}$$

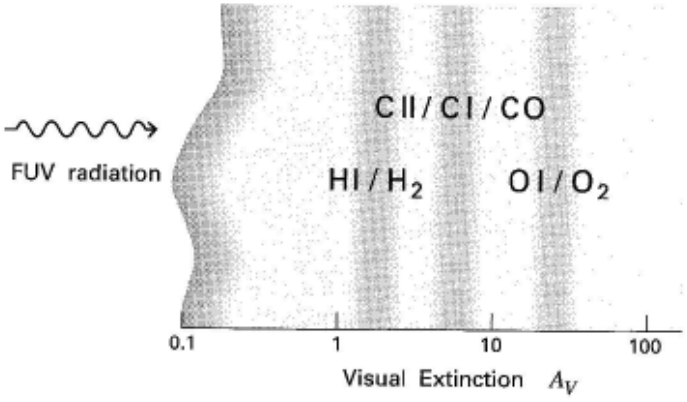

Figure 8.4 – Molecular formation within a cloud as a function of depth (expressed through the visual extinction).

Accordingly, the aforementioned large amount of extinction encountered at these densities implies that the dust will not be appreciably heated by optical radiation. The cooling of the gas into the dust then becomes the main source of heating for the latter. Radiation emanating from the dust grain at longer wavelengths, however, will generally escape the interior of the cloud without any difficulty; this is still the main cooling mechanism for the dust. We then have

$$\Gamma_{\mathrm{d}\to\mathrm{g}} = \Lambda_{\mathrm{d}}. \tag{8.35}$$

Equations (8.34) and (8.35) can be solved simultaneously for T_{g} and T_{d} as a function of the hydrogen density n_{H}. The result of such analysis is presented in Figure 8.5. We see that the high-density temperature profiles shown in Figure 8.2 are thus modified as the rise in the gas temperature stops and eventually declines to a value similar to that of the dust (≈ 4 K) at $n_{\mathrm{H}} \gtrsim 10^6$ cm^{-3}, where the coupling between the two populations is very high. The cut-off in incident ultraviolet and optical photons is responsible for the significant drop in dust temperature from the 16 K shown in Figure 8.1.

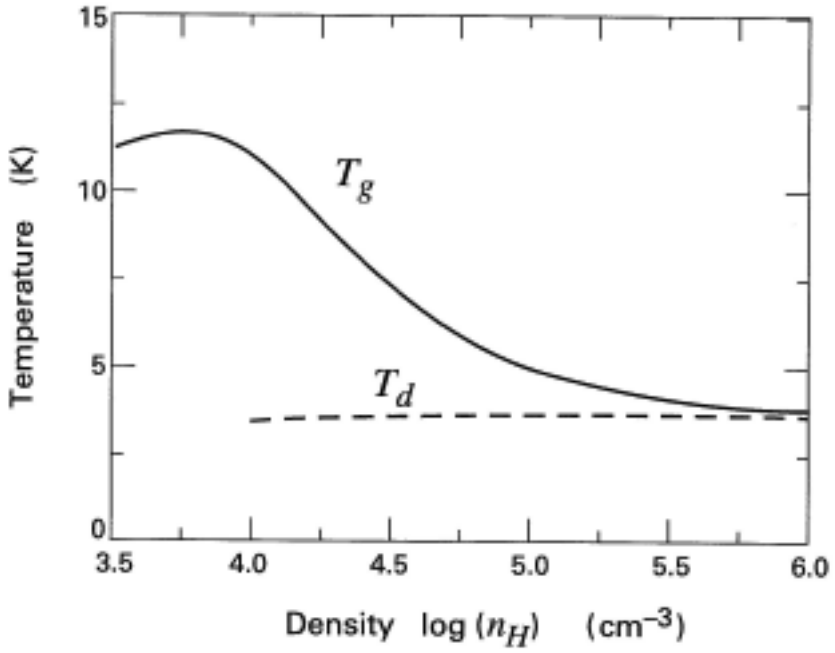

Figure 8.5 – Gas and dust temperatures in the denser regions of a molecular cloud.

8.2.1 **The Ionization Level**

We have already seen that cosmic rays are the main source of ionization in the molecular interior of clouds. It is of considerable interest to evaluate the **ionization fraction**

$$\left[\mathrm{e}^{-}\right] \equiv \frac{n_{\mathrm{e}^{-}}}{n_{\mathrm{H}}}, \tag{8.36}$$

where $n_{\mathrm{e}^{-}}$ is the **electron abundance**. This quantity is fundamental in determining the amount of coupling between the ambient magnetic field and the overall gas. The ionization fraction is usually measured by observing molecular ions such as HCO^{+} (electrons are, of course, undetectable). The sequence of chemical reactions, including the cosmic ray ionization of H_2, that leads to the formation of this molecule is as follows

$$\begin{aligned} \mathrm{CR} + \mathrm{H}_2 &\rightarrow \mathrm{H}_2^{+} + \mathrm{e}^{-} \\ \mathrm{H}_2^{+} + \mathrm{H}_2 &\rightarrow \mathrm{H}_3^{+} + \mathrm{H} \\ \mathrm{H}_3^{+} + \mathrm{CO} &\rightarrow \mathrm{HCO}^{+} + \mathrm{H}_2 . \end{aligned} \tag{8.37}$$

Correspondingly, H_3^{+} is mainly destroyed through its reaction with CO while HCO^{+} is destroyed by **dissociative recombination** with electrons

$$\begin{aligned} \mathrm{H}_3^{+} + \mathrm{CO} &\rightarrow \mathrm{HCO}^{+} + \mathrm{H}_2 \\ \mathrm{HCO}^{+} + \mathrm{e}^{-} &\rightarrow \mathrm{CO} + \mathrm{H}. \end{aligned} \tag{8.38}$$

If we assume chemical equilibrium, i.e., that molecular creation and destruction rates are equal, then we can evaluate the relative abundance of HCO^{+} to n_{H} as

$$\left[\mathrm{HCO}^{+}\right] = \frac{k_2\left[\mathrm{H}_3^{+}\right][\mathrm{CO}]}{k_{\mathrm{dr}}\left(\mathrm{HCO}^{+}\right)\left[\mathrm{e}^{-}\right]}, \tag{8.39}$$

where $k_2 = 2\times10^{-9}$ cm^3 s^{-1} and $k_{\mathrm{dr}}\left(\mathrm{HCO}^{+}\right) = 3\times10^{-6}$ cm^3 s^{-1} are the reaction rates at a temperature of 10 K for equations (8.38), respectively. In the same manner we can write

$$\left[\mathrm{H}_3^{+}\right] = \frac{k_1\left[\mathrm{H}_2^{+}\right]}{k_2[\mathrm{CO}]}, \tag{8.40}$$

where $k_1 \simeq 2\times10^{-9}$ cm^3 s^{-1} (the reaction rate for the creation of H_3^{+} in the second of equations (8.37)), also at 10 K. It is also desirable to do away with $\left[\mathrm{H}_2^{+}\right]$ in equation (8.40), as it is not an observable quantity. Since this abundance is due to the ionization of molecular hydrogen by cosmic rays $\zeta\left(\mathrm{H}_2\right)$ and the corresponding destruction through the first two of equations (8.37), respectively, we write

$$\left[\mathrm{H}_2^{+}\right] = \frac{\zeta\left(\mathrm{H}_2\right)}{k_1 n_{\mathrm{H}}}. \tag{8.41}$$

Inserting equations (8.40) and (8.41) in equation (8.39) we find that

$$\left[\mathrm{e}^{-}\right]=\frac{\zeta\left(\mathrm{H}_{2}\right)}{k_{\mathrm{dr}}\left(\mathrm{HCO}^{+}\right)\left[\mathrm{HCO}^{+}\right]n_{\mathrm{H}}}. \tag{8.42}$$

Using typical values for dense cores (i.e., $\zeta\left(\mathrm{H}_{2}\right)\approx 3\times10^{-17}$ s^{-1}, and $\left[\mathrm{HCO}^{+}\right]\approx10^{-8}$ when $n_{\mathrm{H}}\approx10^{4}$ cm^{-3}) yields a value of $\left[\mathrm{e}^{-}\right]\approx10^{-7}$.

This value for ionization fraction and its dependence on the hydrogen density can also be investigated theoretically. The latter is easily guessed through the realization that the rate at which ions and electrons will recombine must obey the relation

$$\text{recombination rate}\propto n_{\mathrm{e}^{-}}n_{\mathrm{i}}\simeq n_{\mathrm{i}}^{2}, \tag{8.43}$$

where global charge neutrality of the gas was assumed (n_{i} is for the volume density of ions). Furthermore, with our usual requirement of equilibrium, in this case between the cosmic ray ionization of H_{2} and recombination rates, we have

$$\zeta\left(\mathrm{H}_{2}\right)n_{\mathrm{H}_{2}}\propto n_{\mathrm{i}}^{2}. \tag{8.44}$$

Because $\zeta\left(\mathrm{H}_{2}\right)$ is presumably constant with density, we then find that

$$n_{\mathrm{i}}\propto n_{\mathrm{H}_{2}}^{1/2}\simeq\left(\frac{n_{\mathrm{H}}}{2}\right)^{1/2}. \tag{8.45}$$

A more precise analysis shows that

$$\left[\mathrm{e}^{-}\right]=1\times10^{-5}n_{\mathrm{H}}^{-1/2} \tag{8.46}$$

for $n_{\mathrm{H}}\leq10^{8}\mathrm{cm}^{-3}$. This relation is often expressed using the ion and neutral mass densities with

$$\rho_{\mathrm{i}}=C\rho_{\mathrm{n}}^{1/2}, \tag{8.47}$$

where $C=3\times10^{-16}$ cm$^{-3/2}$ g$^{1/2}$. This dependency of the ion density with the square root of the hydrogen density is not made apparent in equation (8.42). This apparent discrepancy between the two analyses would presumably be resolved by carefully accounting for the variation of $\left[\mathrm{HCO}^{+}\right]$ with n_{H}. Equations (8.42) and (8.47) are expected to hold for densities such that $n_{\mathrm{H}}\lesssim10^{8}$ cm^{-3}.